JOURNAL OF MATERIALS SCIENCE 27 (1992) 3435–3441

# Oxidation behaviour of $2\frac{1}{4}$Cr–1Mo steel with prior tempering treatments at 998 K for different durations

R. K. SINGH RAMAN, J. B. GNANAMOORTHY
*Metallurgy Division, Indira Gandhi Centre for Atomic Research, Kalpakkam 603 102, India*

Normalized $2\frac{1}{4}$Cr–1Mo steel has been tempered at 998 K for durations up to 50 h, and then oxidized in air at 773, 873 and 973 K for a maximum duration of 1000 h. The extent of the prior tempering treatment was found to influence the oxidation behaviour of the steel significantly. In general, the oxidation resistance of the steel decreased with increasing duration of prior tempering. However, a pronounced influence has been observed during oxidation at 973 K, when at the end of a 6 h exposure the specimens with prior tempering for 50 h were found to have a weight gain 2.5 times more than the specimen without prior tempering. From the results of the pre- and post-oxidation analyses of the oxide–alloy matrix interfaces by SEM/EDAX, the observed oxidation behaviour could be attributed to the degree of depletion of free (effective) chromium from the alloy by the precipitation of secondary phases of chromium compounds during tempering for different durations. The secondary precipitates in the specimen tempered for 50 h at 998 K can become enriched in chromium by one order of magnitude more than that in the specimen with no prior tempering. Such a drastic depletion of chromium from the matrix causes the formation of a less protective inner oxide layer during oxidation. Acoustic emission tests carried out to assess the mechanical stability of the scale showed that the 50 h tempered specimen suffered cracking after about 4 h oxidation at 973 K, which results in subsequent enhanced oxidation.

## 1. Introduction

Owing to its adequate mechanical properties, $2\frac{1}{4}$Cr–1Mo ferritic steel is used for applications at moderately high temperatures [1, 2]. In order to confer the desired mechanical properties to the alloy, the normalized (air-quenched) steel is generally tempered at temperatures of 923–1023 K [1–3]. Temperature and duration of tempering govern the morphology, composition and distribution of the secondary phases in the alloy microstructure [4–9]. It is known from published literature [4, 5, 8, 9] that a tempering treatment carried out at temperatures above 973 K for durations exceeding 2 h can cause depletion of free chromium from the alloy matrix to form carbides. A microstructural change that involves either a decrease in effective (free) chromium content or a change in the diffusion rate of chromium to the alloy/oxide interface is known to influence the oxidation resistance of Fe–Cr alloys [10–15]. The influence could be pronounced in the case of $2\frac{1}{4}$Cr–1Mo steel owing to the relatively lower chromium content of the alloy. Depletion of free chromium from the matrix of this low alloy steel may result in the formation of an inner oxide layer with less chromium and hence can render the scale less protective [16, 17]. In our preliminary work on this steel, it was concluded [18] that owing to trapping of chromium as carbides, the specimen tempered previously for 3 h oxidized at a faster rate compared to those tempered up to 2 h. However, due to off-normal in-service conditions leading to localized temperature excursions and hot spots, a component may encounter prolonged tempering at higher temperatures that can cause further depletion of chromium.

The present work was carried out to study the influence of prolonged tempering of the normalized $2\frac{1}{4}$Cr–1Mo steel on its oxidation behaviour in air at temperatures of 773, 873 and 973 K. Optical and electron optical examinations were carried out to characterize the microstructural features of the tempered specimens as well as to investigate the possible correlation between the microstructure and the high-temperature corrosion behaviour of the alloy.

## 2. Experimental procedure

### 2.1. Materials

The chemical composition of the steel used is given in Table I. The material was obtained in the form of a

TABLE I Chemical composition (wt %) of the steel used

| C | Mn | Si | S | P | Cr | Mo | Ni | Fe |
|---|---|---|---|---|---|---|---|---|
| 0.07 | 0.42 | 0.19 | 0.025 | 0.19 | 2.28 | 0.95 | 0.09 | Balance |

0022–2461 

6 mm sheet. Rectangular strips cut from such a sheet were cold rolled to 1 mm thickness. Coupons of 10 mm × 10 mm × 1 mm were cut out of the cold-rolled strips. These coupons were vacuum sealed and normalized at 1223 K for 2 h. Tempering treatments were subsequently given to the normalized alloy at 998 K for 5, 10, 25 and 50 h. The heat-treated and mechanically polished specimens were etched in nital, and examined using optical and electron optical microscopes to characterize the microstructure. EDAX analyses could be carried out only on precipitate particles in the specimen tempered for 50 h, the particle sizes of the precipitates in the other specimens being too small for analysis.

### 2.2. Oxidation tests

Specimens with different tempering treatments were polished up to 1 μm diamond finish, degreased and washed in alcohol before oxidation tests. Oxidation tests for long durations up to 1000 h were conducted in a muffle furnace at 773 K in air. To avoid possible losses due to spallations associated with intermittent cooling to room temperature and weighing the same sample in a long-term test, a fresh specimen from each of the five lots of different tempering treatments was loaded at every intermittent duration of test. Short-term oxidation tests were carried out in air in a Mettler TA1 thermobalance at 873 and 973 K when continuous weight change was determined up to 6 h. Duplicate TG runs were performed for each test. The oxidation tests at the three temperatures were also carried out on the untempered specimens (i.e. only normalized).

### 2.3. Post-oxidation analyses

Oxidized specimens were nickel-coated and mounted on their cross-sections and mechanically polished, followed by mild etching. SEM/EDAX analyses were carried out along the thickness of the mounted specimens to assess the influence of tempering treatments on the composition of the inner layer (Fe–Cr oxides) of the duplex oxide scale. EDAX profiles for iron and chromium were also taken along the scale thickness.

### 2.4. Tests for monitoring acoustic emission (AE)

A sudden increase in oxidation rate after 4 h oxidation at 973 K was observed for the specimens tempered for 25 and 50 h; this prompted AE monitoring which was carried out during 6 h exposure at 973 K in order to compare the stability of the oxide scale growing on the untempered specimen with that of the one tempered for 50 h. A schematic diagram of the experimental apparatus for the AE testing and the details of the test can be found elsewhere [15]. For the present test, the polished specimens spotwelded to a platinum wire (a corrosion-resistant waveguide) were placed in a muffle furnace for isothermal oxidation. The other end of the wire was connected to a piezoelectric transducer. This transducer transmitted the AE signals through a preamplifier to an acoustic emission testing unit (AET-204B) that can monitor the various acoustic emission parameters such as cumulative counts, count rates, events, event rates, etc. These signals were recorded on a strip chart recorder. In the present studies, a fixed threshold voltage of 0.78 V and a total system gain of 98 dB were maintained throughout the experiments. Using a 175 kHz transducer and a 125–250 kHz filter, AE count rate mode was operated.

## 3. Results

### 3.1. Microstructure of the materials

As shown in Fig. 1a the nital-etched microstructure of the normalized $2\frac{1}{4}$Cr–1Mo steel consisted mainly of bainite and polygonal ferrite. Further precipitation of the secondary phases and their coarsening can be seen to have occurred during tempering of the steel at 998 K (Fig. 1). However, as shown in the micrographs in Fig. 1b–e, the degree of precipitation and coarsening depended on the duration of tempering, more markedly for the prolonged treatments, i.e. 25 and 50 h duration. Coarsening of the globular particles that appears to have initiated in the case of specimens tempered for 5 and 10 h, became prominent and widespread when the tempering was continued to 25 and 50 h. SEM observations of the microstructure of the specimen tempered for 50 h (Fig. 2) are in agreement with the results of the optical microscopy. A high Cr/Fe ratio ( ~ 78), as indicated by EDAX analyses of the precipitates in this specimen, shows a high degree of chromium enrichment caused by the prolonged tempering for 50 h.

### 3.2. Effect of tempering on oxidation kinetics

As shown in Fig. 3, during oxidation at 773 K for 1000 h tempered specimens oxidized at a faster rate than the untempered specimen. However, the influence can be seen to be more pronounced in the case of specimens tempered for 25 and 50 h. Oxidation kinetics was parabolic for all the specimens. Similar influence of the prior tempering treatments was observed during oxidation at 873 K for 6 h (Fig. 4). At 973 K after about 4 h exposure, the specimens tempered for 25 and 50 h showed a sudden increase in oxidation rate resulting in a paralinear type of kinetics, whereas the other specimens followed parabolic kinetics (Fig. 5). Owing to this increase in the rate, at the end of the 6 h exposure, the 50 h tempered specimens were found to have a weight gain as much as 2.5 times higher than the untempered specimen.

### 3.3. Post-oxidation analyses of scales

Results of the SEM/EDAX examinations across the oxide scale/alloy cross-sections provided useful and conclusive information.

Keeping in mind the influence of the different tempering treatments on oxidation behaviour (Figs 3 and 5), SEM/EDAX examinations were carried out on the oxidized specimens without any prior tempering,

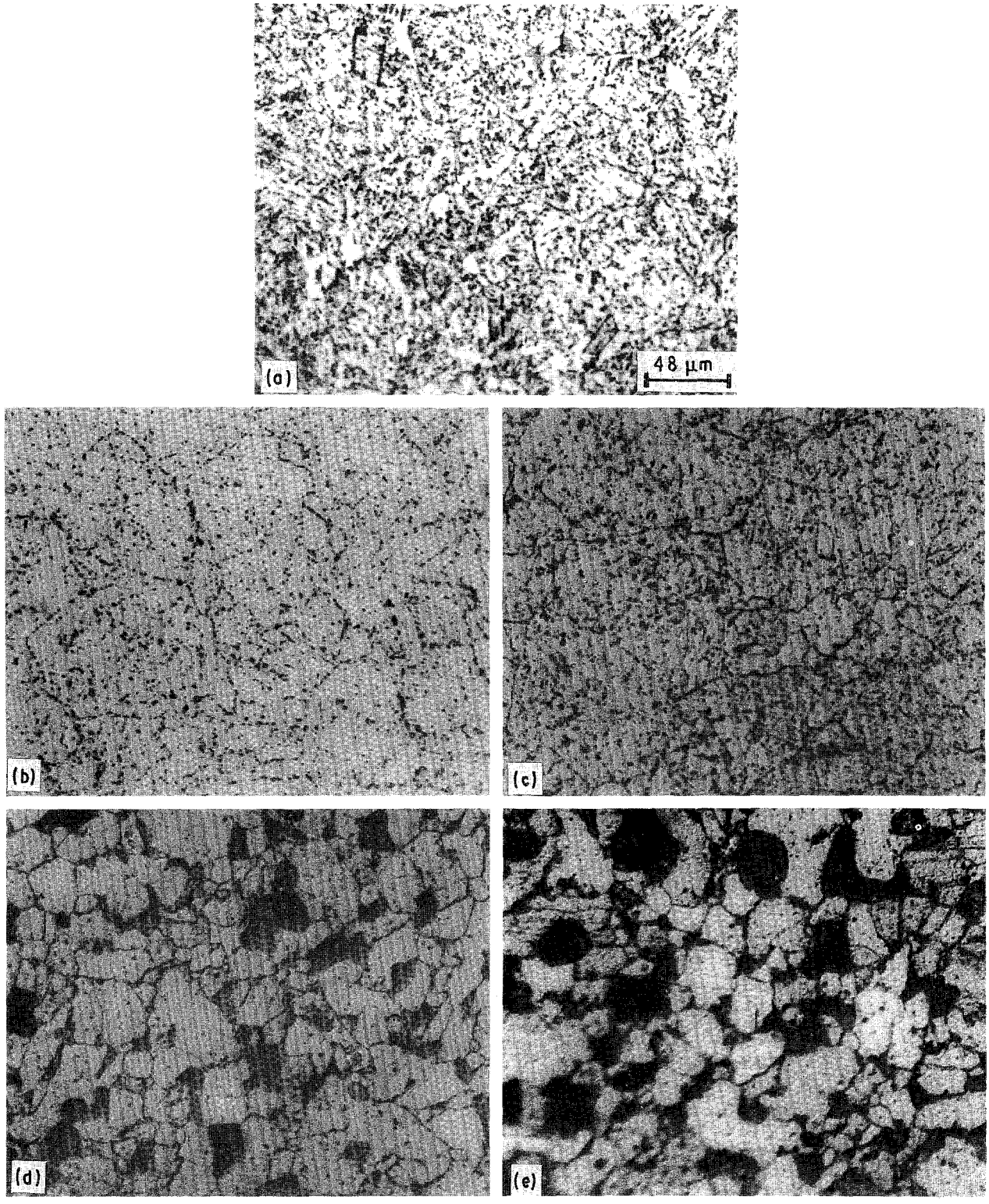


*Figure 1* Optical micrographs of the etched microstructures of a normalized $2\frac{1}{4}$Cr–1Mo steel tempered at 998 K for (a) 0 h (no tempering), (b) 5 h, (c) 10 h, (d) 25 h and (e) 50 h.

and on the specimens tempered for 5 and 50 h. Scanning electron micrographs are given in Figs 6 and 7 and EDAX results in Table II. The micrographs of the specimens oxidized at 973 K (Fig. 7) show that the scale on the 50 h tempered specimen was much thicker than that on the specimen without tempering. Further, the results of the EDAX analyses given in Table II suggest that the chromium content of the inner scale (adjacent to the oxide/alloy interface) of the specimens tempered for 50 h was considerably lower than either of the other two. However, the chromium content of the inner scale of the untempered specimen was appreciably higher than that of the specimen tempered for 5 h.

The chromium content of the inner oxide scales (Fig. 6) of the specimens oxidized at 773 K for 1000 h shows a similar trend, as seen in Table II.

### 3.4. Acoustic emission tests

Results of AE tests during the isothermal oxidation at

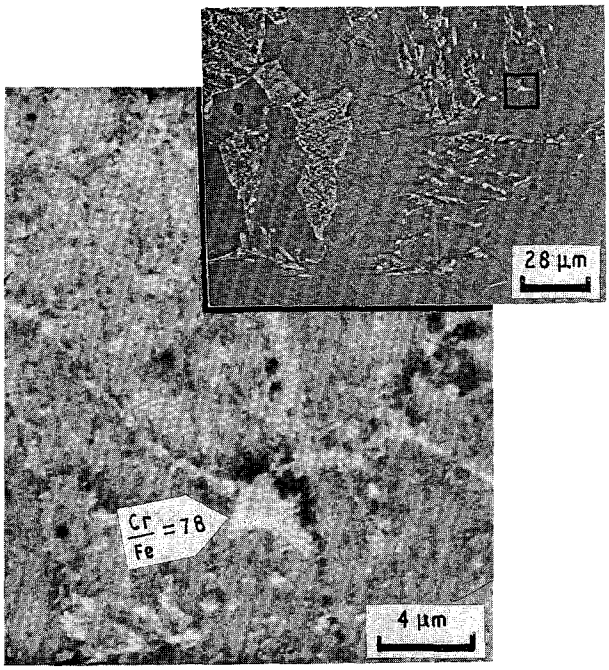


*Figure 2* Scanning electron micrographs of the microstructure of a normalized $2\frac{1}{4}$Cr–1Mo steel tempered at 998 K for 50 h: lower micrograph indicates the high chromium content of a precipitate (EDAX analyses) located in the area marked in the upper micrograph.

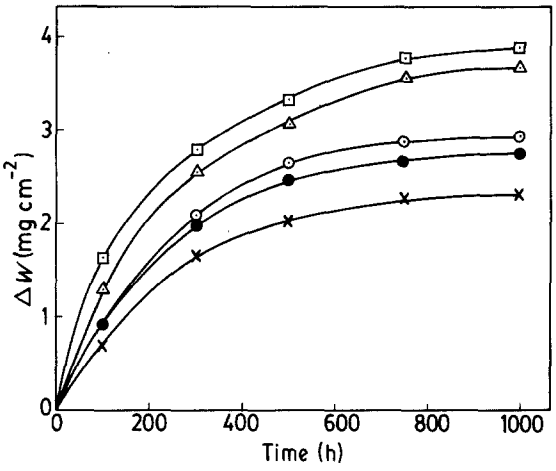


*Figure 3* Weight gain versus time plots for oxidation at 773 K (1000 h) of normalized $2\frac{1}{4}$Cr–1Mo steel tempered previously at 998 K for (×) 0 h, (●) 5 h, (⊙) 10 h, (△) 25 h, (⊡) 50 h.

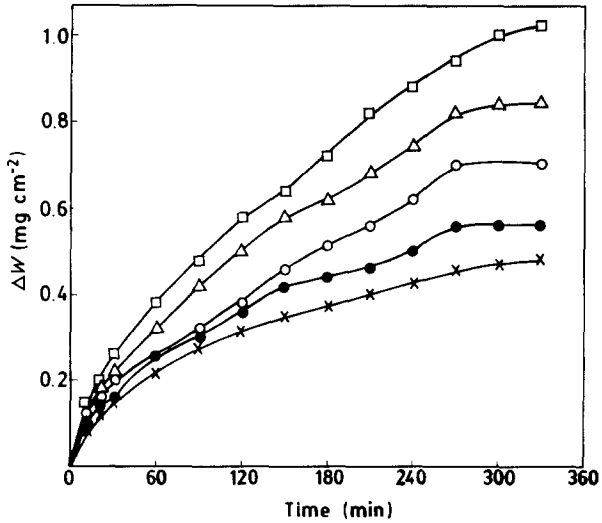


*Figure 4* Weight gain versus time plots for oxidation at 873 K (6 h) of normalized $2\frac{1}{4}$Cr–1Mo steel tempered previously at 998 K for (×) 0 h (no tempering), (●) 5 h, (○) 10 h, (△) 25 h, (□) 50 h.

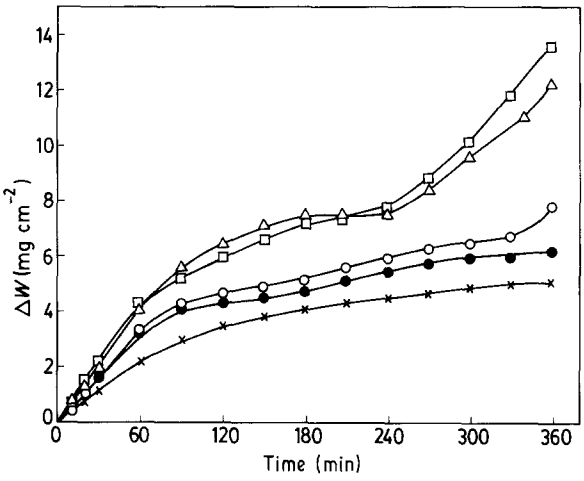


*Figure 5* Weight gain versus time plots for oxidation at 973 K (6 h) of normalized $2\frac{1}{4}$Cr–1Mo steel tempered previously at 998 K for (×) 0 h (no tempering), (●) 5 h, (○) 10 h, (△) 25 h, (□) 50 h.

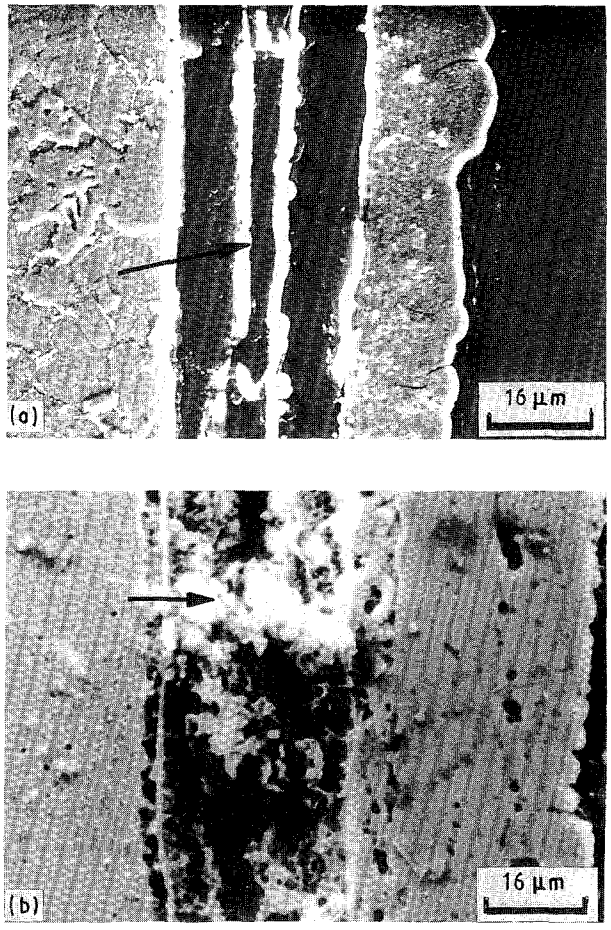


*Figure 6* Scanning electron micrographs of the cross-sections of the oxide scales formed at 773 K (1000 h oxidation) on $2\frac{1}{4}$Cr–1Mo steel with prior tempering at 998 K for (a) 0 h (no tempering) and (b) 50 h. Arrowheads indicate the layers for which the EDAX analyses are given in Table II.

973 K of the tempered (50 h) and untempered specimens are shown in Fig. 8. During the first couple of hours of oxidation, the AE activity from the tempered specimen was only marginally higher compared to that from the untempered one. After about 3 h a sudden increase in AE signals was detected. However,

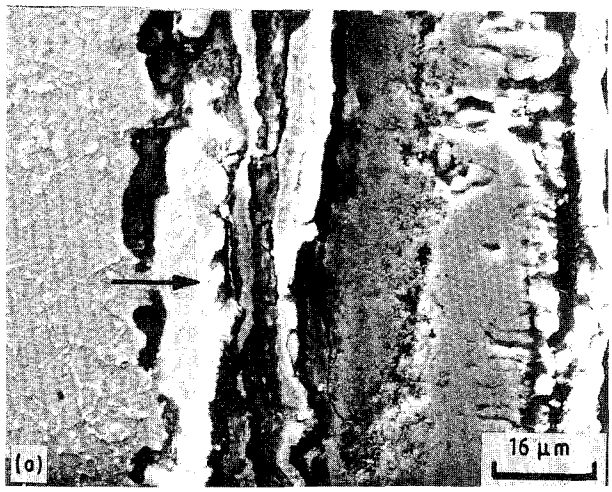


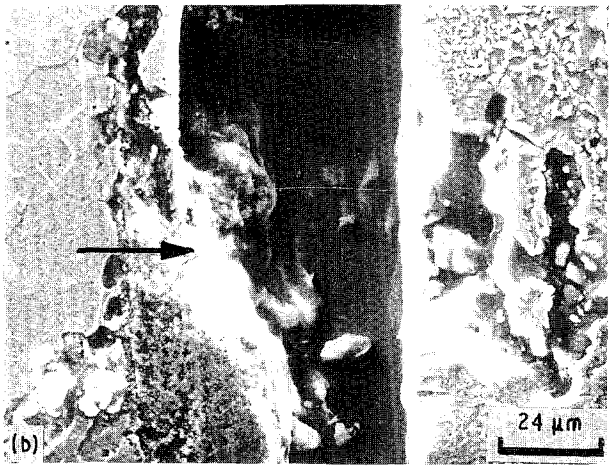


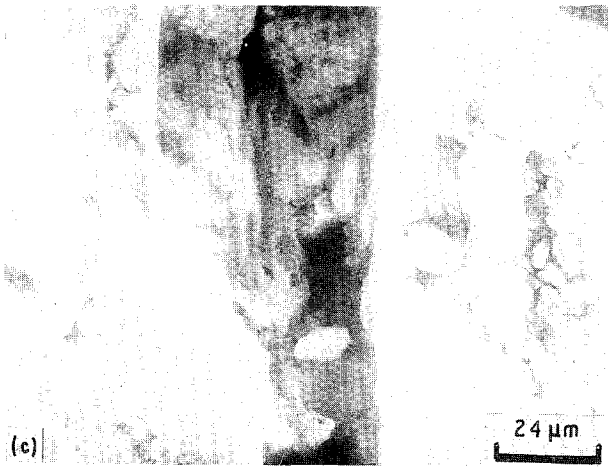


*Figure 7* Scanning electron micrographs of the cross-sections of the oxide scales formed at 973 K (6 h oxidation) on $2\frac{1}{4}$Cr–1Mo steel with prior tempering at 998 K for (a) 0 h (no tempering), and (b, c) 50 h; (c) shows formation of three layers due to repeated rupture in the outer scale. Arrowheads indicate the layers for which the EDAX analyses are given in Table II.

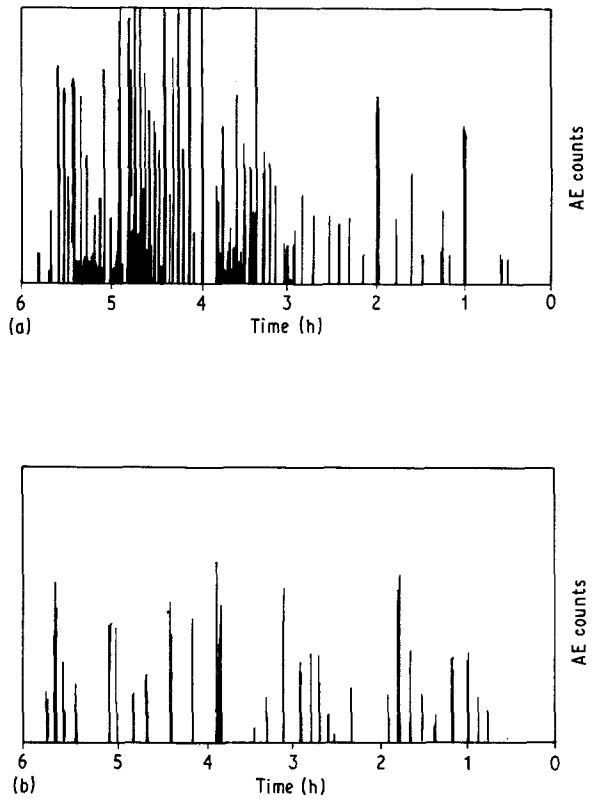


*Figure 8* AE count rate (per 0.25 s) versus time plots during oxidation at 998 K of (a) tempered (50 h) and (b) untempered (only normalized) $2\frac{1}{4}$Cr–1Mo steel.

a preponderent AE activity after about 4 h exposure marked the oxidation behaviour of the tempered specimen that distinctly indicated the mechanical instabilities associated with this scale. It may be worthwhile to note that this higher AE activity from the 50 h tempered material corroborates well with the kinetic curves for oxidation at 973 K (Fig. 5) as well as with the thicker scale formed on this specimen (Fig. 7c).

## 4. Discussion

The oxidation resistance of chromium-containing steels is known to be influenced by the chromium content of the inner scale of Fe–Cr oxides [10–15].

The chromium content of the alloy scale depends on the effective (free) chromium content of the alloy matrix, which is, in turn, influenced by the depletion of free chromium within the matrix due to precipitation as carbides.

According to Baker and Nutting [4] whose work on

TABLE II Chromium contents of the inner layer of the duplex oxide scales formed during oxidation of the normalized $2\frac{1}{4}$Cr–1Mo steel tempered for different durations

| Oxidation temp. (K) | Duration of oxidation (h) | Tempering time (h) | Averaged Fe/Cr ratio in the inner scale |
|---|---|---|---|
| 973 | 6 | 50 | 17.4 |
| | | 5 | 9.8 |
| | | 0[a] | 6.1 |
| 773 | 1000 | 50 | 16.8 |
| | | 5 | 10.7 |
| | | 0[a] | 7.2 |

[a] Specimens with no prior tempering (i.e. only normalized).

$2\frac{1}{4}$Cr–1Mo steel was one of the earliest and most cited, the schematic sequence of carbide precipitation during tempering of $2\frac{1}{4}$Cr–1Mo steel can be summarized as follows.

In bainite

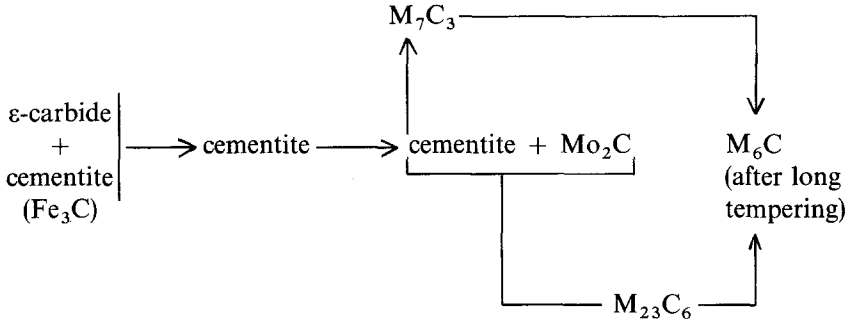


In ferrite

$$Mo_2C \longrightarrow M_6C$$

Among several further investigations in this line [5–9] that have mostly served to confirm the findings of Baker and Nutting [4], a recent investigation due to Pilling and Ridley [9] suggests that, unlike in the earlier scheme, both the chromium-based carbides, $M_{23}C_6$ and $M_7C_3$, nucleate simultaneously in bainite, after the ε-carbide and cementite dissolve in the very early stages of tempering. Early precipitation of $M_{23}C_6$, as suggested in the revised scheme, will incorporate corresponding alterations in the phase fields of the isothermal diagram of Baker and Nutting [4]. The modified diagram, as shown schematically in Fig. 9, is significantly relevant here for the likely additional precipitation of chromium as $M_{23}C_6$, as suggested by Pilling and Ridley [9]. The differences in the microstructural features of the specimens tempered for various durations at 998 K (Fig. 1a–e) can be explained by this diagram.

Secondary phases present in the microstructure of the normalized steel (Fig. 1a) contains ε-carbides and cementite. ε-carbide dissolves in the very early stages of tempering ( ~ 30 min) and is replaced by $Mo_2C$, and the chromium-rich carbides, $M_{23}C_6$ and $M_7C_3$, at the various stages of tempering, as suggested by the schematic diagram in Fig. 9. As is evident from the diagram, all four tempering treatments correspond to the same phase field, that comprises $M_{23}C_6$ and $M_7C_3$ as the major constituents of the secondary phases. However, the degree of precipitation and hence the chromium-depletion from the alloy matrix increased with the duration of tempering (Figs 1b–e and 9). Prolonged tempering may have depleted the majority of free chromium from the matrix, as is evident from the widespread occurrence, and very high chromium content, of the precipitated carbides present as the secondary phases in the specimen tempered for 50 h (Fig. 2). Influence of this depletion is manifested through the very poor oxidation resistance of the 50 h tempered specimen.

Oxidation behaviour of the specimens can be explained in the light of the above-mentioned scheme of the microstructural changes and the results of the post-oxidation analyses by SEM/EDAX. Owing to the extensive depletion of free chromium from the matrix to form $M_{23}C_6$ and $M_7C_3$ upon tempering for 50 h at 998 K (Figs 2 and 9), relatively less protective inner scales (high Fe/Cr ratios) were formed during oxidation of these specimens (Table II, and Figs 6 and 7). Hence, the protection provided by the inner scales on the specimens tempered for 25 and 50 h was much inferior and these specimens oxidized at faster rates (Figs 3–5). A lower degree of precipitation in the case of the specimens tempered for 5 and 10 h allowed formation of a relatively good protective scale (Table II) and oxidation at lower rates. It is obvious from Fig. 9 that an untempered (only normalized) specimen has hardly suffered any chromium depletion from the alloy matrix and, therefore, the oxides in the inner

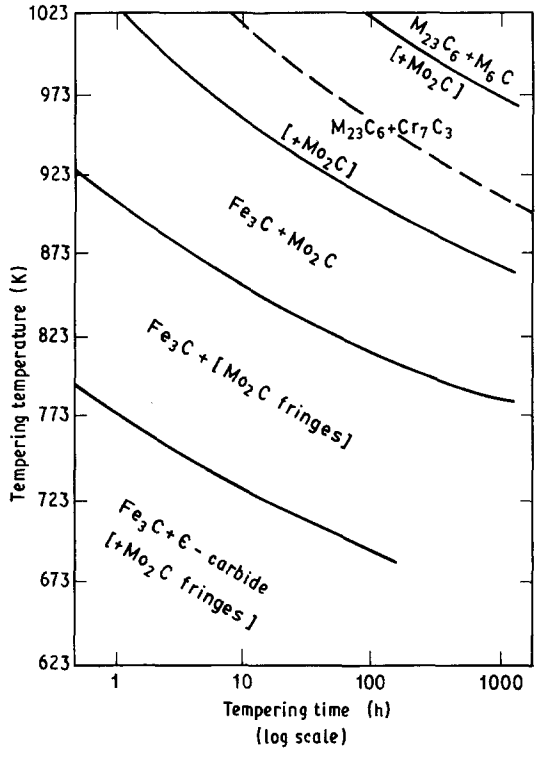


*Figure 9* Isothermal diagram (modified) showing the sequence of carbide precipitation on tempering the normalized $2\frac{1}{4}$Cr–1Mo steel.

scales on these specimens were much higher in chromium content, resulting in oxidation at lower rates. However, depletion of some chromium as carbides, during oxidation at 973 K, cannot be ruled out.

The availability of free chromium in the solid solution can influence the oxidation resistance of $2\frac{1}{4}$Cr–1Mo steel. This can be substantiated by the observed fact that a specimen tempered for 50 h at 998 K showed a marked decrease in the oxidation rate if it was again given the normalizing treatment before the oxidation test, to release more chromium into solid solution through redissolution of carbides formed earlier during tempering. Results of AE tests on 50 h tempered and untempered specimens (Fig. 8) provide the unambiguous signature of the oxidation kinetics of the two specimens at 973 K (Fig. 5). A sudden increase in oxidation rate after 4 h oxidation of the former (50 h tempered) can therefore be ascribed to the mechanical instabilities in the rapidly growing scale on this specimen. The higher oxidation rate produces sufficient thickness in the scale over 4 h to initiate cracks in it, and with much less protective layer underneath (inner layer of Fe–Cr oxide layer) there results a sudden increase in oxidation rate. However, the present behaviour is in contrast to the results of the earlier studies in this laboratory on $2\frac{1}{4}$Cr–1Mo steel where the break-away type of oxidation was detected only at temperatures above 1173 K [13]. But this anomaly finds an explanation in the fact that in the earlier studies no alloy with such a high degree of chromium-depleted matrix was used (only cold-worked and normalized materials were used). Hence, owing to the protective inner scale formation, the overall scale never grew thick enough to suffer from cracking/spallation at lower temperatures.

## 5. Conclusions

The results of the oxidation tests in air at 773 K up to 1000 h, and at 873 and 973 K for 6 h show that the oxidation resistance of the normalized $2\frac{1}{4}$Cr–1Mo steel was influenced in the following manner by the tempering of the alloy at 998 K for 5, 10, 25 and 50 h.

1. Oxidation resistance of the normalized alloy decreased as the duration of tempering was increased from 5 h to 50 h.

2. Influence of prior tempering was more pronounced in the case of specimens tempered for 25 and 50 h.

3. This behaviour was due to the formation of a less-protective oxide scale on the tempered specimens.

4. As assessed by acoustic emission tests, during oxidation at 973 K, the thicker scale formed on the 50 h tempered specimens suffered from mechanical instabilities resulting in sudden increase in subsequent oxidation.


## Acknowledgements

The authors thank Dr Placid Rodriguez, Head, Metallurgy and Materials Programme, for his keen interest and encouragement, and also Mrs M. Radhika for assistance in SEM/EDAX examinations.


## References


1. "Proceedings of BNES International Conference on Ferritic Steels for Fast Reactor Steam Generators", edited by S. F. Pugh and E. A. Little (BNES, London, 1978).
2. "Application of $2\frac{1}{4}$Cr–1Mo steel for Thick-Walled Pressure Vessel", ASTM STP 755 (American Society for Testing and Materials, Philadelphia, PA, 1982).
3. B. J. CANE and R. S. FIDLER, in "Proceedings of BNES International Conference on Ferritic Steels for Fast Reactor Steam Generators", edited by S. F. Pugh and E. A. Little (BNES, London, 1978) p. 193.
4. R. G. BAKER and J. NUTTING, *JISI* **192** (1959) 257.
5. M. MURPHY and G. BRANCH, *ibid.* **209** (1971) 546.
6. T. WADA and G. T. ELDIS, ASTM STP 755 (American Society for Testing and Materials, Philadelphia, PA, 1982) p. 343.
7. J. LEITNAKER, R. L. KLUEH and W. R. LAING, *Met. Trans.* **6A** (1975) 1949.
8. J. ORR, F. R. BECKITT and G. D. FAWKES, in "Proceedings of BNES International Conference on Ferritic Steels for Fast Reactor Steam Generators", edited by S. F. Pugh and E. A. Little (BNES, London, 1978) p. 91.
9. J. PILLING and N. RIDLEY, *Metall. Trans.* **13A** (1982) 557.
10. Y. SHIDA, N. OHTSUKA, J. MURAYAMA, N. FUJINO and H. FUJIKAWA, in "Proceedings of JIMIS-3: High Temperature Corrosion", supplement to *Trans. Jpn Inst. Metals* **63** (1983) p. 631.
11. R. K. SINGH RAMAN, A. S. KHANNA and J. B. GNANAMOORTHY, *J. Mater. Sci. Lett.* **9** (1990) 353.
12. M. K. HOSSAIN, *Corros. Sci.* **19** (1979) 1031.
13. A. S. KHANNA, PhD thesis, Madras University (1985).
14. R. K. SINGH RAMAN, A. S. KHANNA and J. B. GNANAMOORTHY, in "Proceedings, Microscopy of Oxidation", edited by M. J. Bennett and G. W. Lorimer, Cambridge, March 1990, p. 58.
15. R. K. SINGH RAMAN, A. S. KHANNA, B. K. CHOUDHARY and J. B. GNANAMOORTHY, *Mater. Sci. Engng (A)* **148** (1991) 299.
16. N. J. SIMMS and J. A. LITTLE, *Oxid. Metals* **27** (1987) 283.
17. N. J. CORY and T. M. HORRINGTON, *ibid.* **27** (1987) 237.
18. R. K. SINGH RAMAN, A. S. KHANNA and J. B. GNANAMOORTHY, *ibid.* **30** (1988) 345.



*Received 2 July 1988*
*and accepted 3 January 1991*